

RESEARCH

Open Access

Thymoquinone attenuates tumor growth in Apc^{Min} mice by interference with Wnt-signaling

Michaela Lang^{1,2}, Melanie Borgmann^{1,2}, Georg Oberhuber³, Rayko Evstatiev^{1,2}, Kristine Jimenez^{1,2}, Kyle W Damann^{1,2}, Manuela Jambrich^{1,2}, Vineeta Khare^{1,2}, Christoph Campregher^{1,2}, Robin Ristl⁴ and Christoph Gasche^{1,2*}

Abstract

Background: Patients with familial adenomatous polyposis (FAP) are at increased risk for the development of colorectal cancer. Surgery and chemoprevention are the most effective means to prevent cancer development. Thymoquinone (TQ) is considered the main compound of the volatile *Nigella sativa* seed oil and has been reported to possess anticarcinogenic properties. In this study we evaluated the chemopreventive properties of TQ in a mouse model of FAP.

Methods: APC^{Min} mice were fed with chow containing 37.5 mg/kg or 375 mg/kg TQ for 12 weeks. H&E stained intestine tissue sections were assessed for tumor number, localization, size, and grade. Immunohistochemistry for β -catenin, c-myc, Ki-67 and TUNEL-staining was performed to investigate TQ's effect on major colorectal cancer pathways. TQ's impact on GSK-3 β and β -catenin were studied in RKO cells.

Results: 375 mg/kg but not 37.5 mg/kg TQ decreased the number of large polyps in the small intestine of APC^{Min} mice. TQ induced apoptosis in the neoplastic tissue but not in the normal mucosa. Furthermore, upon TQ treatment, β -catenin was retained at the membrane and c-myc decreased in the nucleus, which was associated with a reduced cell proliferation in the villi. *In vitro*, TQ activated GSK-3 β , which induced membranous localization of β -catenin and reduced nuclear c-myc expression.

Conclusions: In summary, TQ interferes with polyp progression in Apc^{Min} mice through induction of tumor-cell specific apoptosis and by modulating Wnt signaling through activation of GSK-3 β . *Nigella sativa* oil (or TQ) might be useful as nutritional supplement to complement surgery and chemoprevention in FAP.

Keywords: *Nigella sativa*, Thymoquinone, Chemoprevention, Colon cancer, Familial adenomatous polyposis

Background

In developed countries, colorectal cancer is one of the most common types of cancer, ranking 2nd and 3rd in women and men respectively. The lifetime risk for colorectal cancer development in the general population is approximately 6% and is responsible for about 8% of all cancer deaths worldwide [1]. Certain familial syndromes are at increased risk for the development of colorectal cancer. This is about 80% in hereditary nonpolyposis

colorectal cancer and almost 100% in familial adenomatous polyposis (FAP) [2].

FAP is an autosomal dominantly inherited disease caused by a germline mutation of the adenomatous polyposis coli gene (APC) located on chromosome 5q21 [3,4]. It is characterized by the development of numerous, predominantly large intestinal adenomatous polyps, ultimately leading to colorectal cancer [2]. Besides endoscopic surveillance and prophylactic surgery, chemoprevention is the most effective means to repress cancer development in FAP. Inhibition of polyp progression improves tumor outcome, thereby prolonging survival in FAP patients. The protective effect of non-steroidal anti-inflammatory drugs (NSAIDs) such as aspirin [5], sulindac [6,7] and the selective cyclooxygenase-2 inhibitor

* Correspondence: christoph.gasche@meduniwien.ac.at

¹Department of Medicine III, Division of Gastroenterology and Hepatology, Medical University of Vienna, Vienna, Austria

²Christian Doppler Laboratory for Molecular Cancer Chemoprevention, Medical University of Vienna, Vienna, Austria

Full list of author information is available at the end of the article

celecoxib [8] has been extensively studied in FAP patients. Some also reduce rectal polyp burden after colectomy with ileorectal anastomosis [6]. Celecoxib was shown to be beneficial against the duodenal tumor burden [9]. However, a chemoprevention study dealing with genotypically but not phenotypically affected patients treated with sulindac failed to show prevention of primary adenoma development [7]. Unfortunately, these drugs are associated with gastrointestinal (bleeding, ulceration) and cardiovascular side effects (thromboembolic events and heart failure) in the long-term [10-12].

In consideration of such side effects, the use of natural substances such as curcumin, eicosapentaenoic acid, apple polyphenols, capsaicin, or thymoquinone (TQ) for chemoprevention is emerging [13-15]. TQ is the main active component of the volatile *Nigella sativa* (black cumin) seed oil, which is used as a spice in countries with low incidence of colorectal cancer such as Egypt, Pakistan, or India. Traditional medicine has utilized its anti-inflammatory, antioxidant, and anti-carcinogenic properties, supporting TQ as a promising dietary chemopreventive agent [16]. *In vitro* studies indicate that TQ inhibits tumor cell proliferation in various cancers [17-19], including colorectal cancer [20,21]. TQ induces a G1 cell cycle arrest, increases p53 and p21WAF1 protein levels, induces apoptosis in a dose- and time-dependent manner, and reduces Bcl-2 protein in HCT116. Further actions of TQ include inhibition of angiogenesis, endothelial cell migration, invasion, and tube formation as demonstrated in HUVECs [18]. *In vivo* weekly i.p. injections of 5mg/kgbw TQ reduced the number and size of aberrant crypt foci and tumor multiplicity in a chemically-induced colorectal cancer mouse model. The suppression of tumor development was sustainable, as treatment with TQ resulted in a reduction of tumor number even after a 10-week discontinuation. Furthermore, in a HCT116 cell xenograft model, a 3-times weekly i.p. injection of 20 mg/kg TQ reduced the relative tumor size by 29% from 2.8 to 2.0 mm² [20]. This study was designed to test the chemopreventive effect of TQ in *Apc*^{Min} (APC, adenomatous polyposis coli; Min, multiple intestinal neoplasia) mice, which best resemble the FAP phenotype.

Results

TQ attenuates tumor growth in *Apc*^{Min} mice

To evaluate the effect of TQ on polyp formation in the *APC*^{Min} mouse, 4–6 week old female and male animals were randomly divided into 4 groups and treated over a period of 12 weeks. Neither TQ nor piroxicam influenced weight gain and food uptake (Additional file 1: Figure S1). Mouse colonoscopy at week 9 demonstrated a significant reduction of distal large intestinal polyps in the TQ-low and the piroxicam group ($p < 0.05$), with

a trend also for TQ-high ($p = 0.124$; Additional file 2: Figure S2).

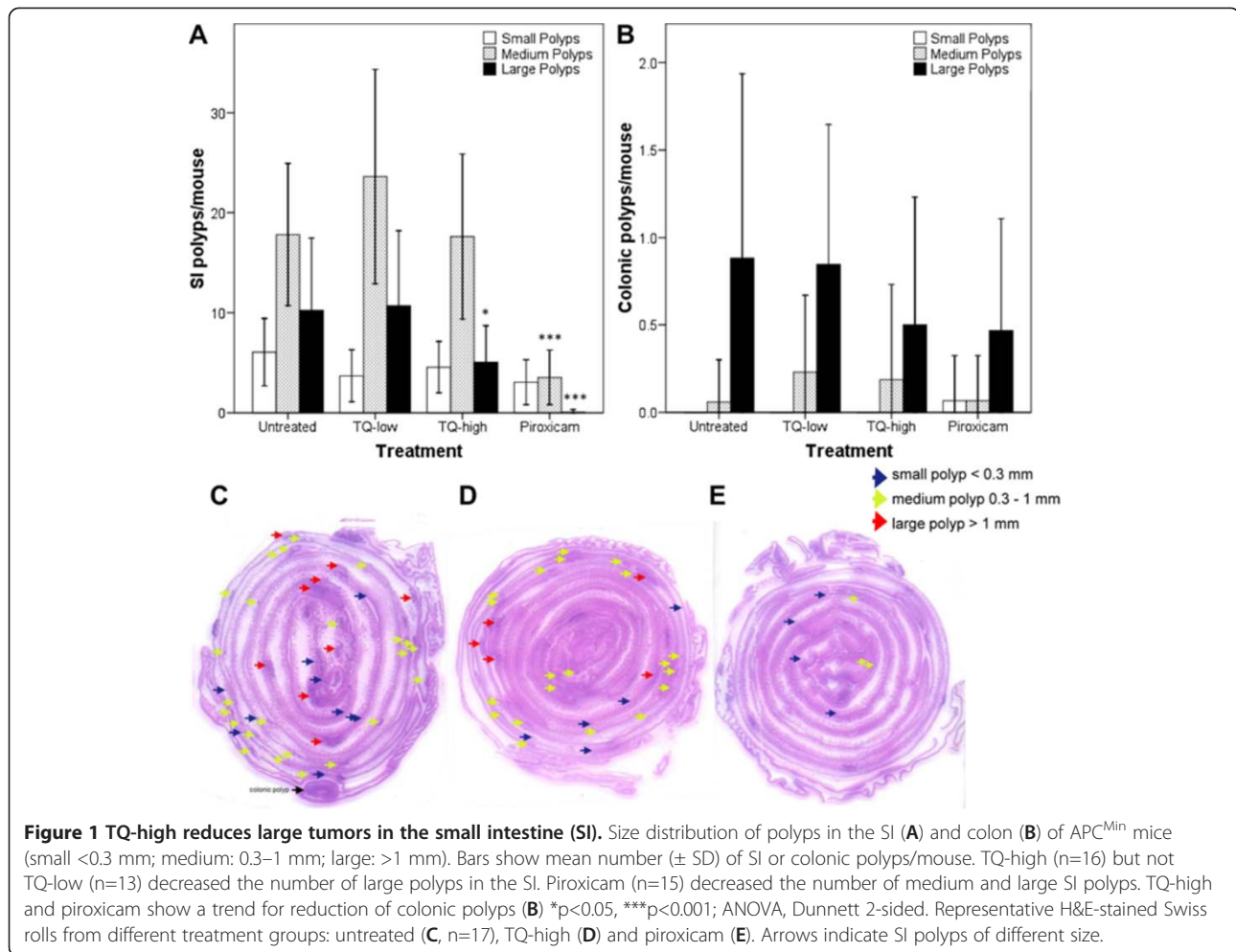
At 12 weeks mice were euthanized and intestinal Swiss rolls were analyzed for tumor number, size (Additional file 1: Figure S1C), and localization (colonic or small intestine). TQ-high decreased the number of large polyps (>1mm) in the small intestine from 10 (95% CI 8–13) to 5 (2–8; $p < 0.05$), while small and medium-sized polyps were unchanged (Figure 1). Tumor multiplicity changed minimally, from 34 (29–40) in untreated *APC*^{Min} mice and 38 (32–44) in TQ-low to 27 (21–33) in TQ-high mice ($p = 0.22$; Additional file 2: Figure S2C). Piroxicam decreased medium-sized polyps from 18 (14–22) to 4 (0–7), large polyps from 10 (8–13) to 0 (-3-3) and tumor multiplicity from 34 (29–40) to 7 (1–13) as expected (Figure 1). Colonic polyp numbers revealed no significant differences between the treatment groups (Figure 1B). A trend was observed for the reduction of colonic polyps within the piroxicam and TQ-high treated groups. Adenocarcinoma formation in the small intestine, defined as penetration of the muscularis mucosae, was found in 1 out of 13 mice in the TQ-low group and in 1 out of 16 mice in the TQ-high group (Additional file 1: Figure S1E).

TQ induces apoptosis in polyps of *Apc*^{Min} mice

To ascertain the effect of TQ on apoptosis, TUNEL-staining of Swiss rolls was performed. Apoptotic cells were analyzed within polyps and normal mucosa of the small intestine. The number of apoptotic cells increased in the neoplastic but not in the normal tissue upon TQ treatment (Figure 2). The average number of apoptotic cells within polyps was 18±16 per FoV for untreated, 45±18 for TQ-low and 50±30 for TQ-high treated mice ($p < 0.05$ and $p < 0.01$, respectively). However, this effect was not observed in the piroxicam treated group (13±14 per FoV). These results suggest that TQ reduces polyp growth through selective induction of apoptosis.

TQ reduces proliferation in the villi of *Apc*^{Min} mice

Nuclear Ki-67 staining was assessed to investigate the effect of TQ on cell proliferation. The percentage of Ki-67 positive cells was scored in polyps, normal crypts and villi of *APC*^{Min}. Neither TQ nor piroxicam altered the number of Ki-67 cells in polyps or crypt cells (Additional file 3: Figure S3). In C57BL/6 wt mice Ki-67 positive cells are specifically restricted to the crypt cells. In *APC*^{Min} mice, however, we observed nuclear Ki-67 staining also in cells of the intermediate zone of the villi. A reduction of Ki-67 positive cells in TQ-high and to a lesser extent also in TQ-low treated mice was observed. The mean Ki-67 IRS in the villi was reduced from 4.8±1.6 to 4.0±1.7 in TQ-low and to 3.6±1.8 in TQ-high ($p < 0.05$) treated cells. Again piroxicam had no effect (IRS 5.1±1.7).



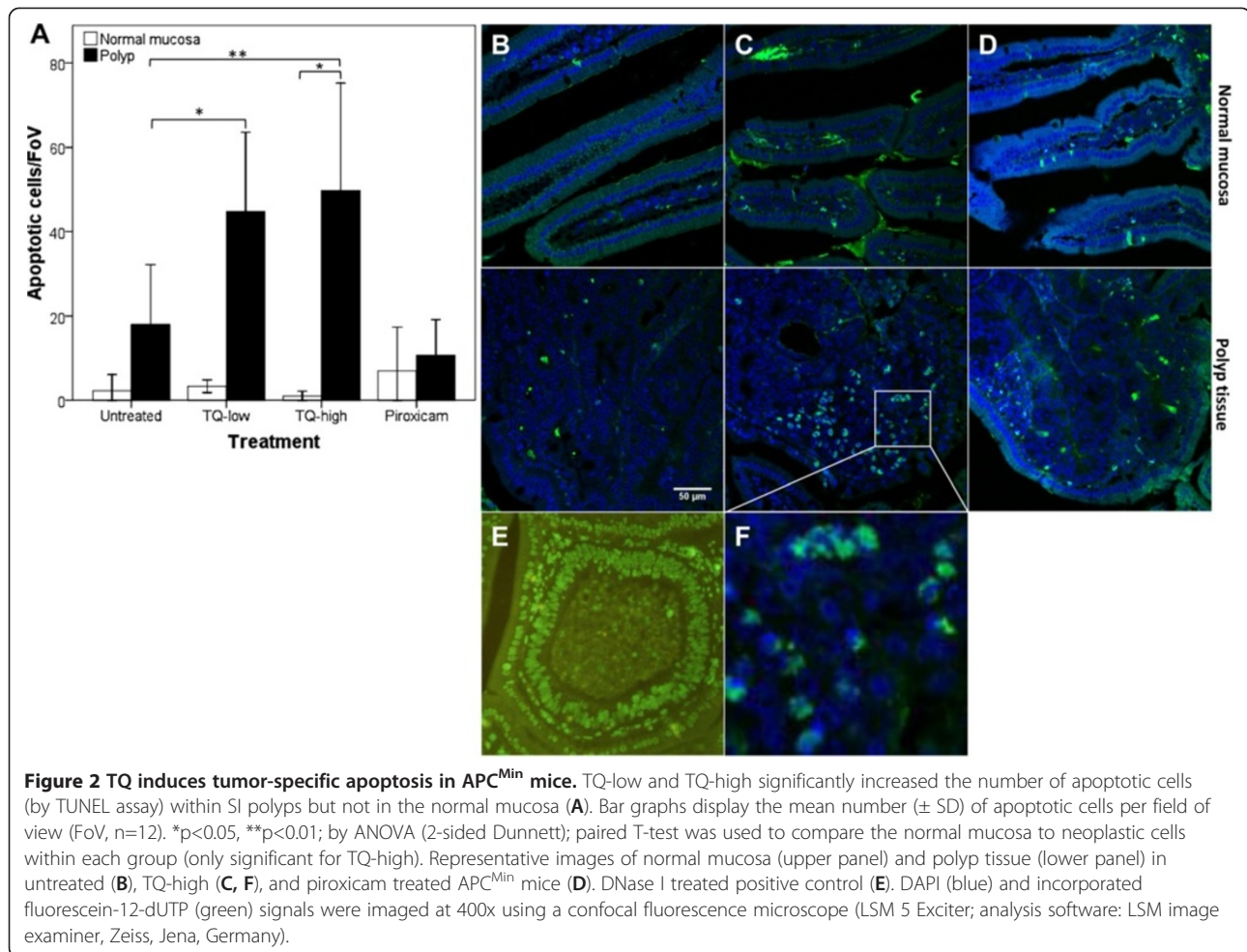
TQ reduces c-myc expression in the polyps of Apc^{Min} mice

We further analyzed nuclear c-myc expression, which is highly abundant in proliferative tissue and necessary for cell cycle progression [22]. TQ-low (p<0.001) and TQ-high (p<0.01) treatment reduced nuclear c-myc protein in the polyps, an effect which was not observed in piroxicam-treated mice (Figure 3).

TQ translocates β-catenin to the membrane in APC^{Min} polyps

As TQ influenced tumor size and c-myc expression, we considered how TQ may be implicated in the β-catenin pathway. Loss of APC protein leads to a deregulated WNT/β-catenin pathway, as APC is part of the β-catenin destruction complex. Deregulated β-catenin degradation leads to an accumulation of free β-catenin and nuclear translocation. In the nucleus, β-catenin acts as a transcription factor binding in a complex with TCF/LEF to DNA enhancer sequences leading to the upregulation of genes like the proto-oncogene c-myc

[23]. A membranous, cytoplasmic, and nuclear IRS was calculated for β-catenin in the normal mucosa, small and large polyps. Remarkably, β-catenin was translocated to the membrane in large polyps of TQ-high treated APC^{Min} mice (p<0.05; Figure 4). A trend towards this effect was seen for small polyps as well (p=0.064). We found a similar trend for β-catenin shifting to the membrane in piroxicam treated mice (p=0.094). No change in β-catenin expression within the normal epithelium was identified, except for a slight increase in cytoplasmic β-catenin levels in TQ-low treated mice, an effect which was abrogated in small and large polyps. To further investigate β-catenin expression upon TQ treatment, we studied the poorly differentiated colon cancer cell line RKO, which harbors wt APC [24], wt p53 [25] and wt β-catenin alleles, the latter being expressed at low levels [24]. Treatment with TQ resulted in decreased nuclear β-catenin within 4 h and up to 24 h (as shown by Western blot). In parallel, membranous and cytoplasmic β-catenin increased at 4 h (Figure 5A). In conclusion, TQ reduces nuclear β-catenin and translocates β-catenin to the membrane.



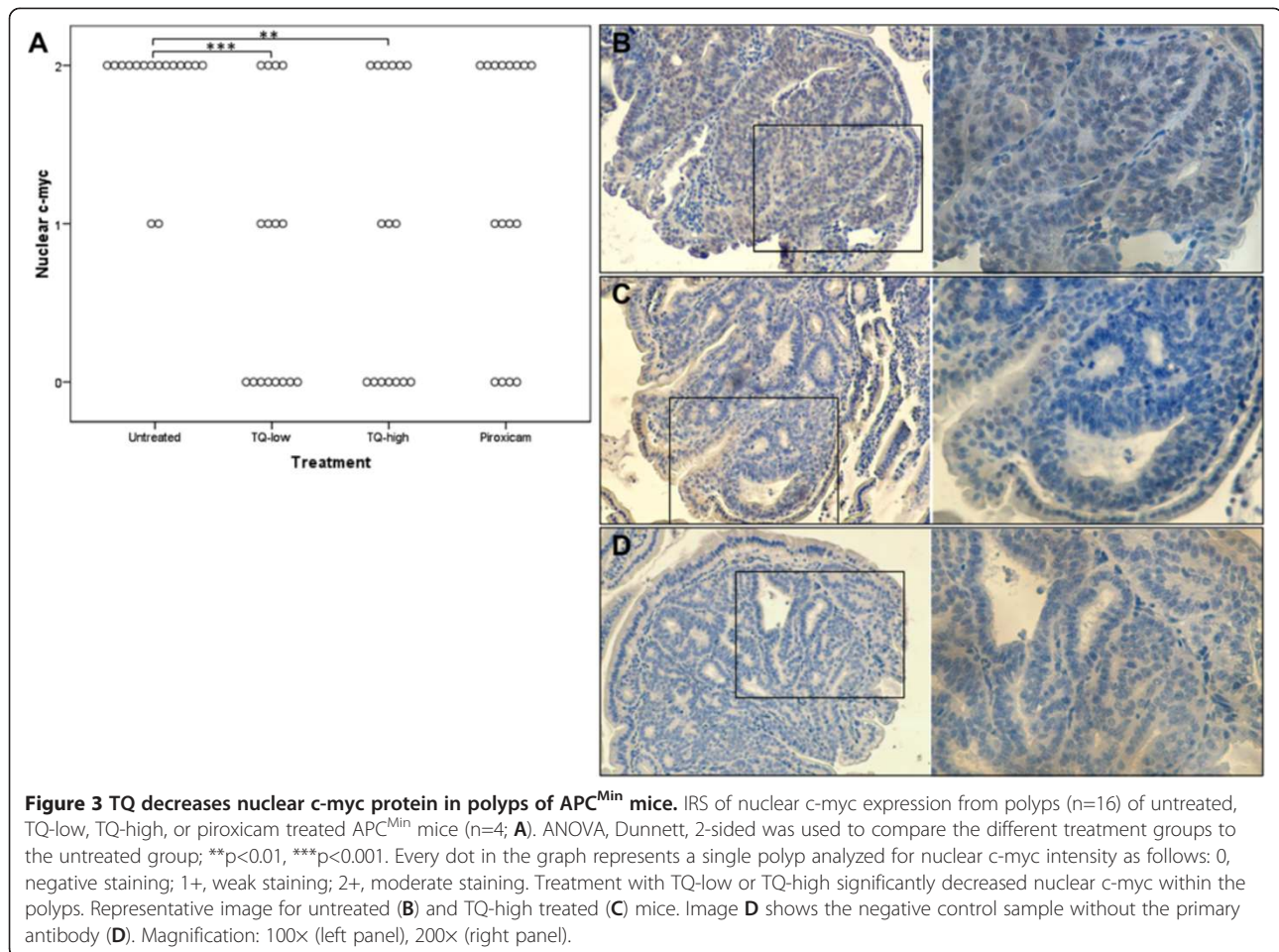
TQ exerts different effects on cell viability on colon cancer cells with various mutational backgrounds

To assess the effect of TQ on cell viability, MTT assays were performed in different human colon cancer cell lines (having various mutational backgrounds) and in HCEC-1CT normal diploid human colon epithelial cells. APC-truncated and p53-mutated cells (DLD1 and HT29) are the most resistant to TQ (IC_{50} : 196 μ M and 160 μ M, respectively). LoVo, which has wt p53 and mutated APC, was the most sensitive, having an IC_{50} value of 36 μ M. In comparison, cells with wt p53 and wt APC such as HCT116, RKO and HCEC-1CT were less affected by TQ, with IC_{50} values of 118, 86 and 79 μ M, respectively (Additional file 4: Figure S4A). These results indicate that TQ's effect on cell viability may be influenced by the mutational status of APC and p53. To provide further evidence that TQ induces cell apoptosis rather than cell cytostasis, RKO cells were incubated with increasing TQ concentrations for 24 h and Annexin V/PI staining was performed. Indeed, TQ treatment led to a concentration dependent increase

in apoptotic and dead cells measured by flow cytometry (Additional file 5: Figure S5).

TQ acts on the GSK-3 β pathway

TQ was reported to inhibit proliferation and angiogenesis by suppressing ERK and AKT phosphorylation in HUVECs [18]. In RKO, ERK1/2 and AKT1 are highly phosphorylated. In our experiments, TQ did not have any effect on the phosphorylation status of ERK1/2 (Thr202/Tyr204) nor AKT1 (Ser473) from 30' to 12h, despite successful inhibition of phosphorylation of ERK1/2 by the MEK1/2 inhibitor UO126 (Additional file 4: Figure S4C and D). A well-known downstream target of the PI3K/AKT pathway and, alternatively, the RAS/RAF/MEK/ERK pathway, is the glycogen synthase kinase 3 β (GSK-3 β). The activity of GSK-3 β is inversely correlated with its phosphorylation status at Ser9. When testing for GSK-3 β phosphorylation upon TQ treatment, we observed a reduction of p-GSK-3 β . GSK-3 β appears to be an important molecular target of TQ, which may subsequently affect the stability of c-myc (Figure 5).



TQ downregulates c-myc protein expression

Active GSK-3 β is assumed to be an important kinase phosphorylating c-myc on Thr58 for subsequent ubiquitination by the F-box protein Fbw7 [26], a component of the SCF-class ubiquitin ligase (E3) complex, and degradation. Indeed, treatment with TQ reduces c-myc expression at 2 h and 24 h (Figure 5A-C). The subcellular distribution of c-myc showed reduced expression of nuclear c-myc upon TQ treatment (Figure 5A), which is in line with the reduced nuclear c-myc expression in polyps of APC^{Min} mice (Figure 3). To further support the mediation of c-myc reduction at protein level, c-myc mRNA was quantified. In fact, the expression of c-myc mRNA was not altered upon TQ treatment (Additional file 4: Figure S4B).

TQ reduces GSK-3 β phosphorylation via inhibition of the MEK1/2 pathway rather than PI3K

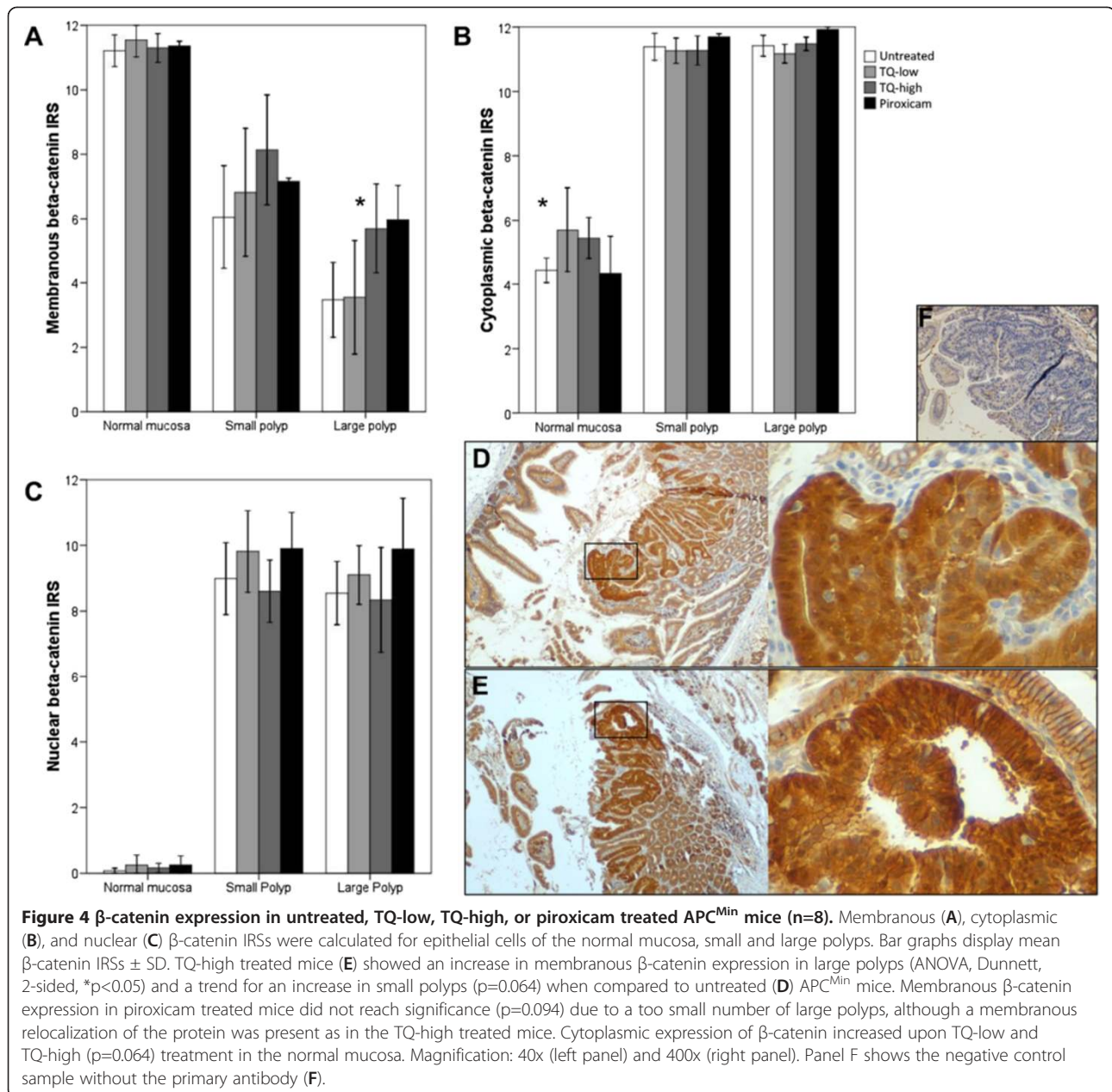
As a next step we verified if the reduced GSK-3 β phosphorylation upon TQ treatment was dependent on the PI3K pathway, which is upstream from GSK-3 β . We used the PI3K inhibitor LY294002 together with TQ to test for synergistic or additive effects. Treatment with

TQ and LY294002 for 2 h and 4 h reduced the levels of GSK-3 β phosphorylation in an additive manner (see also Figure 5D, E, Table 1 and Methods section for statistical explanation) indicating that TQ's effect on GSK-3 β phosphorylation is independent of PI3K. As expected, total GSK-3 β levels remained stable over time. Also, total c-myc protein was reduced more effectively at the 4 h point in time, if both substances have been added (Figure 5D).

We then investigated the RAS/RAF/MEK pathway, which also influences GSK-3 β Ser9 phosphorylation. MEK1/2 inhibition with UO126 and concomitant incubation with TQ did not show additional reduction of GSK-3 β phosphorylation (Figure 5E), assuming that both compounds are utilizing the same pathway. As stated above, pharmacological inhibition of MEK1/2 in RKO cells resulted in an abrogation of p-ERK1/2 phosphorylation that was not seen on treatment with TQ. Therefore, we assume that TQ carries out its function by inhibiting another kinase in this pathway.

Discussion

In this study we demonstrate that TQ, the main active component in the essential oil of *Nigella sativa* seeds,



reduces the number of large polyps in the small intestine of APC^{Min} mice. This effect was mainly due to induction of tumor cell-specific apoptosis. In addition, we found a shift of β -catenin to the membrane and a reduced nuclear c-myc expression in polyps. In RKO, TQ activates GSK-3 β , which in turn might mediate phosphorylation and subsequent degradation of c-myc protein (model see Figure 6).

Black cummin seed oil is commonly used in traditional medicine and as a spice in countries with low prevalence for colorectal cancer [16]. It has been described to interfere with several tumor pathways. Gali-Muhtasib and others showed that TQ reduces the number of aberrant

crypt foci and inhibits tumor growth in a 1,2-dimethylhydrazine-induced and a xenograft colon carcinogenesis mouse model, mainly by induction of apoptosis. Furthermore this group demonstrated that TQ decreases the invasive potential of a mouse colorectal cancer cell line [20]. Other publications showed that the antiproliferative and apoptotic effects of TQ are either mediated by p53-dependent or independent mechanisms. The former could be shown for colorectal cancer cells, the latter only for osteosarcoma cells [27] and a myeloblastic leukemia cell line [28]. p53-null HCT116 cells were less sensitive to TQ-induced growth arrest and apoptosis compared to p53-wt HCT116 cells [21]. The reduced

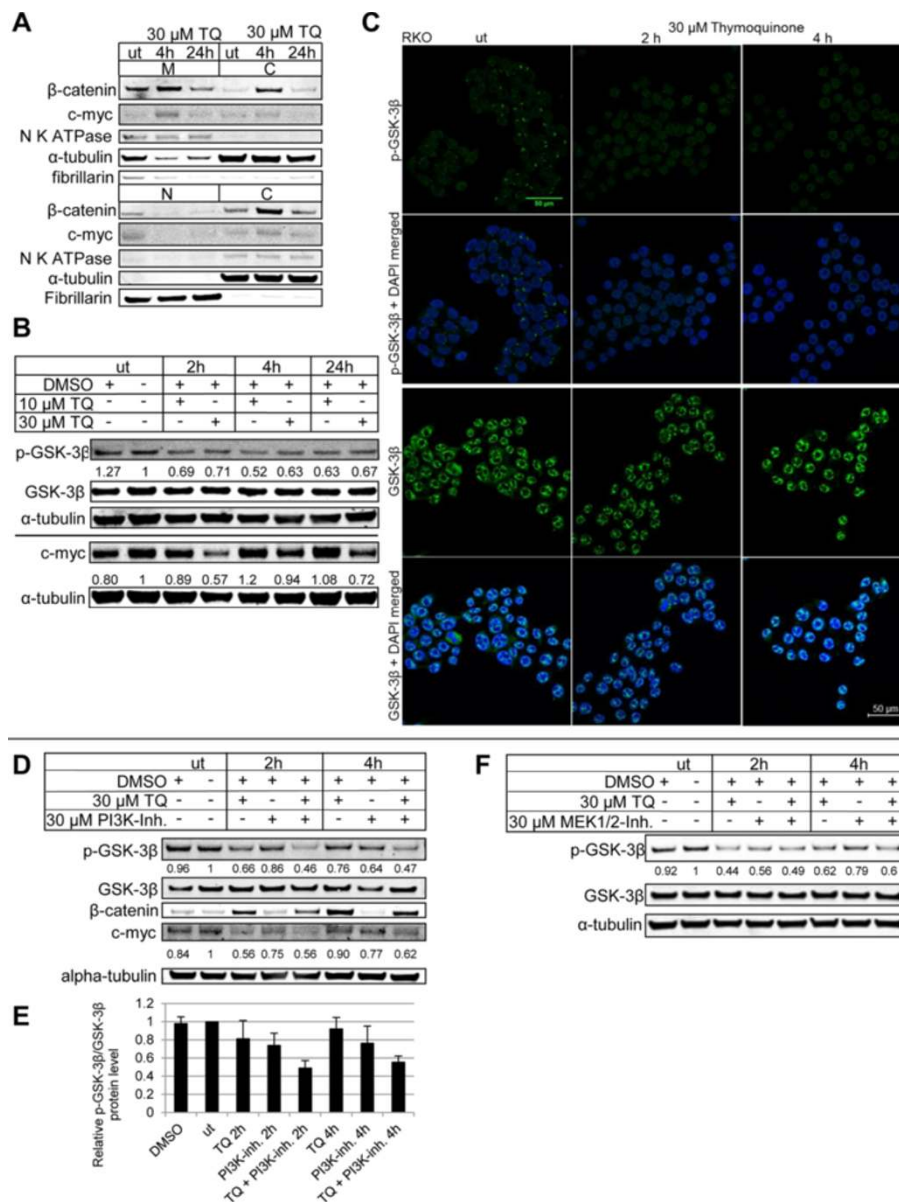


Figure 5 Effect of TQ on β-catenin and the glycogen synthase kinase 3β (GSK-3β) pathway in RKO. Separating for membranous, cytoplasmic and nuclear protein fractions showed reduction of nuclear β-catenin and c-myc upon 30 μM TQ for up to 24 h and a short term increase of membranous and cytoplasmic β-catenin. α-tubulin is used as a total protein and cytoplasmic marker, fibrillarlin as nuclear marker, and Na-K-ATPase as membranous marker (A). TQ reduces the amount of p-GSK-3β Ser9, the inactive form of the protein, at concentrations of 10 and 30 μM, shown by Western blot (B) and fluorescence microscopy (C, top panel, green: p-GSK-3β, blue: DAPI; LSM 700). Total GSK-3β protein levels are constant over time (B; C, bottom panel). Total c-myc levels were reduced at 30 μM TQ up to 24 h, an effect that was not seen for 10 μM (B). 30 μM TQ and 30 μM PI3K inhibitor LY294002 additively reduced the amount of p-GSK-3β in total protein lysates. 5 independent Western blots had been carried out and the ratio of p-GSK-3β levels and total GSK-3β protein has been calculated with densitometry analysis (D, E and see also Table 1 for the statistical calculations). Treatment with TQ increased total β-catenin protein but reduced the amount of c-myc protein (D). Inhibition of MEK1/2 with 30 μM UO126 reduced p-GSK-3β, while concomitant incubation with TQ did not lead to an additive reduction of p-GSK-3β (F).

apoptosis in p53^{-/-} HCT116 cells is due to an up-regulation of the DNA damage sensor CHK1, which is normally transcriptionally repressed by p53 [29]. This is in line with our observation that cells having functional p53, such as LoVo, HCEC-1CT, RKO and HCT116,

are more sensitive to TQ induced cell death compared to cells with p53 mutations, as shown for DLD1 and HT29. Also, we could confirm in our model that one of the main chemopreventive pathways of TQ is the cancer cell-specific induction of apoptosis which is

Table 1 GSK-3β dephosphorylation

Treatment	Experiment					Experiment 1-5 AVG of [1] -[2] (±SD)
	1	2	3	4	5	
DMSO	1.06	0.91	0.96			
ut	1.00	1.00	1.00	1.00	1.00	
2 h	TQ	0.90	0.87	0.66	0.47	
	PI3K-inh.	0.69	0.84	0.86	0.57	
	[1] TQ + PI3K-inh.	0.61	0.47	0.46	0.41	
	[2] Multiplication of TQxPI3K-Inh.	0.61	0.73	0.56	0.27	
Difference [1] -[2] at 2 h	-0.01	-0.26	-0.10	0.15		-0.06 (±0.17)*
4 h	TQ	0.93	1.07	0.76		0.92
	PI3K inh.	0.67	1.04	0.64		0.69
	[1] TQ + PI3K inh.	0.59	0.53	0.47		0.62
	[2] Multiplication of TQxPI3K-Inh.	0.62	1.11	0.49		0.63
Difference [1] -[2] at 4 h	-0.03	-0.59	-0.02		-0.01	-0.16 (±0.28)**

RKO cells were treated with TQ, PI3K inhibitor or with a combination of both substances for 2 h or 4 h to test for synergistic or additive effects on the dephosphorylation of GSK-3β. 5 different Western blots were performed and the relative ratios of p-GSK-3β and total GSK-3β protein levels were calculated using the program Image J. Mathematically, when effects are measured as proportions, the additive effect of two substances is the multiplication of the two values resulting from the single treatments. The mathematical product of both treatments is only minimally deviating from the actual values for the double treatment resulting from the Western blots. The null-hypothesis of no mean difference cannot be rejected at either time point (T-test, p-value *0.56 (2 h) and **0.34 (4 h)). While this result is in itself no proof of additivity, a closer inspection of the calculated differences shows that the assumption of additivity is indeed reasonable: In experiments 1, 3 and 5 the differences are very close to zero. Experiments 2 and 5 show stronger deviations, however in opposite directions and the resulting mean differences are close to zero for both time points.

likely mediated by p53. TQ was shown to induce oxidative stress and subsequently H2AX phosphorylation in HCT116 cells, which was diminished in p53^{-/-} HCT116 [29]. The authors concluded that the changes in H2AX expression and the increased apoptosis correlated with enhanced mitochondrial ROS production. In addition to TQ's tumor cell-specific induction of apoptosis we

observed that TQ reverses the Ki-67 positivity found in the cells of the intermediate zone of APC^{Min} villi. This is indicative of lowered proliferation in the normal tissue. However, the number of Ki-67 was not altered in polyps. This result is in agreement with previous studies that assessed Ki-67 staining in HCT116 xenograft tumors [20].

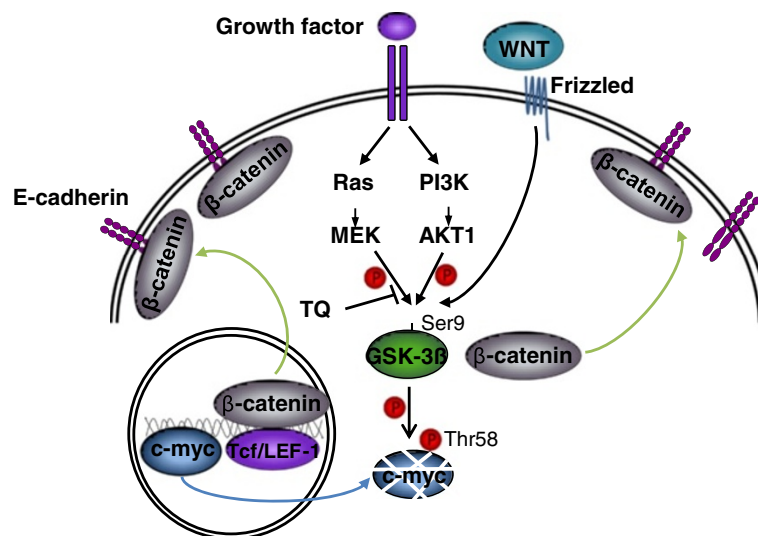


Figure 6 A model of TQ's effect on colon cancer cells. In untreated colorectal cells GSK-3β is phosphorylated on Ser9 by various pathways (Ras-Raf-MEK, PI3K-AKT1, WNT), and thereby inactivated. This allows accumulation of β-catenin in the cytoplasm, its nuclear translocation and activation of Tcf/LEF-1. Thymoquinone (TQ) treatment reduces GSK-3β Ser9 phosphorylation (downstream of Ras, Raf, MEK) leading to a relocalization of β-catenin to the membrane (green arrows) and reduction of nuclear c-myc (likely via phosphorylation, ubiquitination and subsequent degradation; blue arrow; ref. 37).

In vitro analysis of TQ's influence on the Ser9 phosphorylation status of GSK-3 β , an important kinase for cell differentiation and apoptosis, showed reduced phosphorylation and activation of the protein. There is increasing evidence that c-myc Thr58 is phosphorylated by active GSK-3 β , thereby regulating its stability by mediating Fbw7-driven turnover [26]. Enhanced GSK-3 β activity by TQ might lead to phosphorylation and subsequent degradation of c-myc. The cause of reduced Ser9 phosphorylation in RKO cells is still elusive. Concomitant treatment with TQ and the PI3K inhibitor LY294002 leads to an additive reduction of p-GSK-3 β , assuming that, in colon cells, TQ does not utilize the PI3K/AKT pathway, as shown for prostate cancer [18]. Instead, inhibition of MEK1/2 with UO126 reduced p-ERK1/2 and p-GSK-3 β levels and concomitant treatment with TQ did not reveal an additive effect on GSK-3 β phosphorylation, indicating that TQ mediates its effect over the RAS/RAF/MEK pathway rather than ERK1/2. As shown *in vivo* and *in vitro* TQ leads to membranous β -catenin translocation, which is probably also mediated by GSK-3 β activation. This is in line with a study conducted by Li et. al. showing that active GSK-3 β interacts with MUC1, thereby releasing MUC1 bound β -catenin, which then associates with membranous E-cadherin [30] (Figure 6).

One shortcoming of the study is the limited effect of TQ on tumor multiplicity. In this respect our results deviate from a chemically-induced colorectal cancer model [20]. TQ may have less activity in genetically-driven cancer models such as the APC^{Min} mouse than in chemically-induced models. Another contributing factor might be the administration route of TQ (as part of the chow versus intraperitoneal injections). Also differences in the mutational status of APC may partially explain this phenomenon. We have therefore used RKO cells (APC wt) for *in vitro* studies.

The TQ concentration in seeds is between 0.12 and 0.25% (w/v) [31,32]. In the essential oil, which is about 0.41 - 0.44% of the total seed, the TQ concentration is between 28 - 57% [31]. The human equivalent dose of 375 mg/kg TQ in the diet corresponds to 3.6 mg/kg body weight, resulting in a total amount of 219 mg for a body weight of 60 kg [33]. Studies using TQ in *H. pylori* infection [34] or diabetes [35] report an uptake of up to 3 g *Nigella sativa* seeds/day for one to three months, respectively. Both studies report amelioration of the disease but no severe side effects or adverse effects on renal or hepatic functions, respectively. Assuming a seeds content of 0.2% TQ, this results in an effective dose of 6 mg TQ per day. In mice, no adverse effects except for a decrease in glucose levels was observed with TQ concentrations up to 90 mg/kg body weight [36]. The corresponding concentration in our study was 45 mg/kg

body weight for TQ-high. Thus the concentrations used are likely well tolerated without major toxicity. A dose dependent decrease of GSH levels in vital organs was found only with higher concentrations (2–3 g/kg, p.o.), most probably due to formation of TQ conjugates with GSH (glutathionyl-dihydrothymoquinone), which might affect bioavailability as well as antioxidant properties of TQ [36,37].

In summary, TQ interferes with polyp progression in APC^{Min} mice by inducing tumor cell-specific apoptosis and by modulating Wnt signaling through GSK-3 β activation, β -catenin translocation and reduction of nuclear c-myc. TQ or *Nigella sativa* seed oil might be a useful nutritional supplement to complement current chemoprevention in FAP.

Methods

Mice, genotyping, treatment, and colonoscopy

Heterozygous male C57BL/6J-Apc^{Min}/J (APC^{Min}) mice (The Jackson Laboratory, Bar Harbor, ME) were bred with wild-type female C57BL/6J mice. Apc^{Min} mice harbor a nonsense mutation at nucleotide 2549 in the murine homolog of the human APC gene [38]. Genotyping was performed from mouse tail DNA using primer-introduced restriction analysis-polymerase chain reaction with APC primers (APC_{for}: 5'-TCT CGT TCT GAG AAA GAC AGA AGC T-3'; APC_{rev}: 5'-TGA TAC TTC TTC CAA AGC TTT GGC TAT-3') and HindIII digestion according to Musteanu et al [39]. 4–6 week old female and male APC^{Min} mice were housed at the Institute of Biomedical Research (Medical University Vienna, Vienna). Mice were kept under 12 hour light/dark cycles. Chow and water were available ad libitum. Animals were weighed weekly and the amount of food intake was documented. All animal experiments were performed in accordance with the Austrian and European law, defined by the Good Scientific Practice guidelines of the Medical University Vienna (animal ethics approval number: BMWF-66.009/0113-II/10b/2010).

The animals were randomly divided into 4 groups and treated over a period of 12 weeks. Chemopreventive substances were added to a commercial rodent diet (C1000, Altromin, Lage, Germany) as follows: 37.5 mg/kg chow of TQ (274666, Sigma Aldrich) referred to as TQ-low (n=13) and 375 mg/kg chow of TQ referred to as TQ-high (n=16). 200 mg/kg chow piroxicam (P5654, Sigma-Aldrich) was used as a positive control (n=15) [40,41]. Mice fed the diet alone served as a negative control (n=17). Mice gaining less than 1.5 g of weight were excluded for analysis, as the chemopreventive substance was taken up through the diet. Mice with breast cancer, which is associated with the APC^{Min} phenotype [42], were euthanized and excluded from analysis. At week 9 of treatment mice underwent colonoscopy. Briefly, mice

were anesthetized with an i.p. injection of ketamine and xylazine, the colonoscope (Karl Storz, Tuttlingen, Germany) connected to an airpump (Eheim, Deizau, Germany) was inserted and the colon inflated [43]. During insertion and withdrawal of the colonoscope up to 3 cm the number of polyps was determined in real-time using a standard monitor and a video was recorded. Mice were euthanized, the intestine was dissected, flushed with PBS and 10% neutral buffered formalin, and coiled up to a Swiss roll [44]. Prior to paraffin embedding the intestine was fixed in neutral buffered formalin for 24 h.

Histology, immunohistochemical analysis, and apoptosis

Serial tissue sections (4 μ m) were H&E stained and analyzed by an expert pathologist (G.O.) who was blinded for the treatment group. Polyp number, localization (small intestine, colon), size (small < 0.3 mm; medium 0.3 – 1 mm; large polyp > 1 mm), and tumor grade (adenoma; adenocarcinoma – here defined by the penetration of the muscularis mucosae) were assessed [45]. Apoptosis was determined using the DeadEnd™ Fluorometric TUNEL System (G3250, Promega, Mannheim, Germany). For visualization of nuclei and mounting Vectashield® Mounting Medium with DAPI (H-1200; Vector Laboratories, Burlingame, CA) was used and samples were analyzed by confocal microscopy (LSM 5 exciter; Zeiss Germany).

Immunohistochemical staining was performed on paraffin-embedded mouse intestine using antibodies against β -catenin, Ki-67, c-myc and isotype specific (anti-mouse/anti-rabbit) biotinylated secondary antibody and standard staining procedures (details for antibodies see Additional file 6: Table S1). Slides were dried, dewaxed in xylene and rehydrated using a decreasing alcohol series. After blocking of endogenous peroxidase with 15% H₂O₂ in methanol, antigen retrieval was performed in 10 mM citrate buffer, pH 6. Subsequently, slides were blocked in 2% horse serum, 3% BSA in TRIS buffer and endogenous IgG was blocked with Vector M.O.M. Blocking Reagent (MKB-2213, Vector Laboratories). Primary antibodies were incubated at 4°C overnight, followed by biotinylated secondary antibody and avidin-biotin-HRP complex (Vectastain ABC Kit, PK-6100; Vector Laboratories). Staining was visualized using 3,3'-diaminobenzidine (32750; Fluka) and nuclear counterstaining was performed using hematoxylin. Slides were dehydrated and embedded in Histofluid (6900002; Marienfeld, Lauda Koenigshofen, Germany). Images were recorded at 40 \times to 400 \times magnification using an Olympus BH-2 microscope and an Olympus E330 digital camera. Immunoreactivity was independently scored by two investigators. A standardized immunoreactivity scoring system was modified to evaluate both the intensity of

immunohistochemical staining and the proportion of cells stained [46]. The staining intensity was classified into 0 (no staining), 1+ (weak), 2+ (moderate), 3+ (strong) and the percentage of positive cells was recorded (0-100%), resulting in a highest value of 300. Total counts were divided by 25 to reach a maximum immunoreactivity score (IRS) of 12, to be comparable to other publications using a scoring system reaching a maximum of 12 [46]. IRS was calculated for small polyps, large polyps and normal mucosa of 6 different fields of view (FoV). C-myc staining was evaluated by scoring the overall staining intensity per polyp (n=16) as follows: negative (0), weakly (1+) or moderately positive (2+).

Cell culture and reagents

The human colon cancer cell lines (DLD1, HCT116, HT29, LoVo, and RKO), obtained from ATCC, were cultured in IMDM (Gibco/Invitrogen) supplemented with 10% FBS (Biochrom, Berlin, Germany) and Penicillin-Streptomycin solution (Gibco). The normal diploid human colon epithelial cell line HCEC (1CT) [47], a kind gift from Jerry W. Shay, were cultured as previously described [48]. Cells were incubated at 5% CO₂, 37°C and a relative humidity of 95%. Cells were treated with 10–30 μ M TQ (Sigma-Aldrich; 274666) and/or 30 μ M PI3K inhibitor LY294002 (9901; NEB) or 30 μ M MEK1/2 inhibitor UO126 (9903; NEB) for indicated times.

Immunocytochemistry

Fluorescence immunocytochemistry was performed using antibodies against p-GSK-3 β and GSK-3 β . Cells were fixed, permeabilized, blocked and incubated with the primary antibody overnight at 4°C. For protein visualization secondary AlexaFluor 488 antibody was used (Additional file 6: Table S1). Nuclear counterstaining was performed using Vectashield mounting medium with DAPI. Images were scanned 400 \times magnification on a LSM 700 (Zeiss).

Annexin V/propidium iodide staining

1.5 \times 10⁵ RKO cells were seeded in a 6-well plate and grown for 24 h. Cells were treated with 0–120 μ M TQ for 24 h or 5 μ g/ml Actinomycin D (positive control) for 16 h and processed for Annexin V-FITC/propidium iodide (PI) staining according to the manufacturer's protocol (eBioscience, BMS500FI). Annexin/PI positive cells were measured with a Cell Lab Quanta SC Flow Cytometer (Beckman Coulter) and analyzed with Quanta Analysis software.

Cell viability assay

1.5 \times 10⁴ cells/well were seeded in a 96-well microtiter plate and grown for 24 h. After a 24 h-treatment with 0–500 μ M TQ, cells were incubated for 3 h with 0.5 mg/mL MTT (Sigma, M5655). The cells were subjected

to a 1:1 ethanol/DMSO treatment to dissolve formazan crystals. The intensity of the solubilized crystals was measured colorimetrically at 570 nm (Anthos 2010). Each measurement was performed in biological quadruplicates.

Western blotting

Cells were rinsed with PBS, lysed in ice-cold RIPA buffer, and centrifuged. The protein concentration was determined via Bradford assay and equal protein amounts (25 µg) were boiled in SDS gel sample buffer. Proteins were separated by SDS-PAGE and immunoblotted onto a PVDF membrane. Nuclear and cytoplasmic separation was carried out as published elsewhere [49]. Membranous and cytoplasmic separation was performed as described by Howard et al. [50]. Primary antibodies were used as follows: β-catenin, p-GSK-3β (Ser9), GSK-3β, c-myc, p-ERK1/2 (Thr202/Tyr204), ERK1/2, p-Akt (Ser473), Akt, α-tubulin, Na-K-ATPase, and fibrillarin (Additional file 6: Table S1). Bands were visualized with anti-rabbit or anti-mouse IRDye coupled antibodies and scanned on Odyssey imager (LI-COR). Densitometry was done with ImageJ 1.45 (<http://rsb.info.nih.gov/ij/>).

Quantitative real time-PCR

Total RNA was isolated with TRIZOL reagent (Biorad) and was reverse transcribed to cDNA using the ThermoScript RT-PCR System (11146-024; Invitrogen) according to the manufacturer's protocols. Quantitative real time-PCR was carried out in duplicates using Fast SYBR Green Master Mix (AB; 4385612) and c-myc primers (Additional file 6: Table S2). Data were normalized to two endogenous controls GAPDH and β-actin (QIAGEN). Relative expression levels of the transcripts were calculated using the comparative CT method [51].

Statistics

Statistical analysis was performed using SPSS software version 17.0. Polyp number, size, and the number of apoptotic cells (TUNEL assay) were analyzed using univariate analysis of variance (ANOVA). Results were corrected by Dunnett (2-sided). Paired T-test was used to analyze the number of apoptotic cells in the normal mucosa compared to neoplastic tissue within one group. Immunohistochemistry data for β-catenin, Ki-67 and c-myc staining were analyzed using ANOVA. Results were corrected by Dunnett (2-sided). To investigate the additive or synergistic nature of the effects of TQ and PI3K-inhibitor on GSK-3β dephosphorylation the expected effects under the assumption of additivity were compared to the actual effects measured in the double treatment experiments. Since the effects are measured as proportions, an additive nature of effects means that the expected double effect is the product of the single effects. This product was calculated for each experiment and

point in time and compared to the measured effect of the double treatment by calculating the difference. The resulting differences are reported for all experiments. The mean and the standard deviation of the differences were calculated for 2 h and 4 h points in time. Paired T-tests were performed to test the null-hypotheses of the mean differences being zero. p-values were considered as statistical significant if less than 0.05 (*p<0.05; **p<0.01; ***p<0.001). Data are expressed by mean and the 95% confidence interval for the mean (95% CI) or mean and standard deviation.

Additional files

Additional file 1: Figure S1. Average weight curves [g] of female (A) and male (B) APC^{Min} mice treated with TQ-low (n_{female}=8, n_{male}=5 dashed line), TQ-high (n_{female}=10 n_{male}=6, dots), piroxicam (n_{female}=11, n_{male}=4 dot-dashed line) or left untreated (n_{female}=12, n_{male}=5, line). Representative H&E images of tumors with different size: (I) <0.3 mm/small, (II) 0.3-1 mm/medium, (III) >1 mm/large; 40x (C). Average food intake in grams per mouse a day for each treatment group (D). H&E images of the two adenocarcinomas, defined by penetration of the muscularis mucosae, (arrows) found in the small intestine in the TQ-low (I) and TQ-high (II) treated group; 100x (E).

Additional file 2: Figure S2. Colonoscopy and small intestinal tumor number. Number of polyps/mouse detected during colonoscopy after 9 weeks of treatment, reaching 2-3 cm into the colon (A). Representative images of normal mucosa (I) and polyps of different size (II-IV) are shown (B). For TQ-low (n=14) and piroxicam (n=14) a significantly reduced number of polyps compared to untreated (n=17) mice was found via colonoscopy. For TQ-high (n=17) a trend for reduction of polyps was seen. Every dot represents the number of polyps of a single mouse. *p<0.05; ANOVA, Dunnett 2-sided. Total number of polyps in the SI of APC^{Min} mice (C). Bars show mean number (± SD) of SI polyps/mouse. Piroxicam decreased the total number of SI polyps. For TQ-high there was a trend for reduction of total SI polyps. ***p<0.001; ANOVA, Dunnett 2-sided.

Additional file 3: Figure S3. Proliferation. Ki-67 IRS (A) calculation for villi, crypts and polyps (n=8 each, 4 mice) of untreated (B), piroxicam (C), TQ-low (D) and TQ-high (E) treated APC^{Min} mice. Bar graphs show mean Ki-67 IRSs (± SD). High dose TQ lowered the amount of Ki-67 positive cells in the villi compared to control samples, for low dose TQ there was a trend to that effect (A). Representative images of Ki-67 staining in the small intestine (B-E); upper left panel: normal mucosa; upper right panel: polyp; lower panel: magnification of a single villus. Panel F shows the negative control sample where the primary antibody was omitted (F). *p<0.05; ANOVA, Dunnett, 2-sided was used to compare the different treatment groups to the control group. Magnification: 100x (top panel), 400x (bottom panel).

Additional file 4: Figure S4. MTT assay. TQ exerts different effects on cell viability in cancer cell lines having various mutational backgrounds. Colon cancer cells and 1CT normal diploid human colon epithelial cells were incubated with TQ at different concentrations in quadruplicates for 24 h. The absorbance values (relative OD), expressed as means, compared to untreated cells were measured by MTT assay and IC50 concentrations were calculated (A). TQ does not exert its effect on the p-ERK1/2 and p-AKT1 (Ser473) pathway, but inhibition of MEK1/2 with the compound UO126 at 30 µM abrogated p-ERK1/2 phosphorylation (Thr202/Tyr204) between 30' and 12 h and reduced to a much lower extent p-AKT (Ser473), shown for whole cell lysates of RKO cells (B and D). Colon cancer cell lines RKO and HT29 were treated with 30 µM TQ for indicated times or left untreated (control). C-myc transcript levels stay constant upon TQ treatment. Relative mRNA expression levels of c-myc were calculated with GAPDH and β-actin as endogenous controls using

qRT-PCR and the $\Delta\Delta Ct$ method. Error bars represent standard deviations of technical duplicates (C).

Additional file 5: Figure S5. Annexin V/propidium iodide staining. RKO cells were treated with increasing concentrations of TQ for 24 h (A-E), with 5 $\mu\text{g/ml}$ actinomycin D (positive control) for 16 h (F) or with the DMSO (solvent for TQ) for 24 h (G). The number of viable (lower left quadrant), early apoptotic (lower right quadrant), apoptotic (upper right quadrant) and dead cells (upper left quadrant) was measured on a Cell Lab Quanta SC Flow Cytometer and calculated with the Quanta Analysis software (H). With increasing TQ concentrations the number of apoptotic and dead cells is enriched.

Additional file 6: Table S1. Antibody list; *Immunohistochemistry; **Immunocytochemistry. **Table S2.** qRT-PCR primer list.

Abbreviations

APC: Adenomatous polyposis coli gene; FAP: Familial adenomatous polyposis; FoV: Field of view; IRS: Immunoreactivity score; TQ: Thymoquinone.

Competing interest

The authors disclose no conflicts.

Authors' contributions

ML: Conception and design, acquisition of data, analysis and interpretation of data, writing of the manuscript, MB: Acquisition of data, analysis and interpretation of data. GO: Analysis and interpretation of data. RE: Statistical analysis. KJ: Acquisition of data, analysis and interpretation of data, proof-reading of the manuscript. KWD: Development of methodology, revision of the manuscript. MJ: Technical support, analysis and interpretation of data. VK: Conception and design, interpretation of data, revision of the manuscript. CC: Conception and design, revision of the manuscript. RR: Statistical analysis. CG: Obtained funding, conception and design, study supervision, revision of the manuscript. All authors read and approved the final manuscript.

Acknowledgement

The financial support by the Federal Ministry of Economy, Family and Youth and the National Foundation for Research, Technology and Development is gratefully acknowledged. Confocal images were taken in cooperation with the Institute of Pathology and the Imaging Core Facility of the Medical University of Vienna. We thank Robert Eferl and Monica Musteanu, Ludwig Boltzmann Institute for Cancer Research, Medical University of Vienna, for teaching Swiss roll preparation and the APC^{Min} mouse genotyping protocol.

Funding

The study was supported by the Federal Ministry of Economy, Family and Youth and the National Foundation for Research, Technology and Development. This study was supported in part by the Austrian Science Fund (FWF P24121 to CG).

Author details

¹Department of Medicine III, Division of Gastroenterology and Hepatology, Medical University of Vienna, Vienna, Austria. ²Christian Doppler Laboratory for Molecular Cancer Chemoprevention, Medical University of Vienna, Vienna, Austria. ³Pathology Ueberlingen, Ueberlingen, Germany. ⁴Center for Medical Statistics, Informatics, and Intelligent Systems, Section for Medical Statistics, Medical University of Vienna, Vienna, Austria.

Received: 11 January 2013 Accepted: 7 May 2013

Published: 13 May 2013

References

1. Ferlay J, Shin HR, Bray F, Forman D, Mathers C, Parkin DM: **Estimates of worldwide burden of cancer in 2008: GLOBOCAN 2008.** *Int J Cancer* 2010, **127**:2893–2917.
2. Boyle P, Levin B: **5.7 Colorectal Cancer.** In *World Cancer Report 2008*. 1st edition. Edited by Boyle P, Levin B. Lyon: International Agency for Research on Cancer (IARC); 2008:374–379.
3. Nishisho I, Nakamura Y, Miyoshi Y, Miki Y, Ando H, Horii A, Koyama K, Utsunomiya J, Baba S, Hedge P: **Mutations of chromosome 5q21 genes in FAP and colorectal cancer patients.** *Science* 1991, **253**:665–669.
4. Groden J, Thliveris A, Samowitz W, Carlson M, Gelbert L, Albertsen H, Joslyn G, Stevens J, Spirio L, Robertson M, et al: **Identification and characterization of the familial adenomatous polyposis coli gene.** *Cell* 1991, **66**:589–600.
5. Burn J, Bishop DT, Chapman PD, Elliott F, Bertario L, Dunlop MG, Eccles D, Ellis A, Evans DG, Fodde R, et al: **A randomized placebo-controlled prevention trial of aspirin and/or resistant starch in young people with familial adenomatous polyposis.** *Cancer Prev Res (Phila)* 2011, **4**:655–665.
6. Cruz-Correa M, Hyland LM, Romans KE, Booker SV, Giardiello FM: **Long-term treatment with sulindac in familial adenomatous polyposis: a prospective cohort study.** *Gastroenterology* 2002, **122**:641–645.
7. Giardiello FM, Yang VW, Hyland LM, Krush AJ, Petersen GM, Trimbath JD, Piantadosi S, Garrett E, Geiman DE, Hubbard W, et al: **Primary chemoprevention of familial adenomatous polyposis with sulindac.** *N Engl J Med* 2002, **346**:1054–1059.
8. Steinbach G, Lynch PM, Phillips RK, Wallace MH, Hawk E, Gordon GB, Wakabayashi N, Saunders B, Shen Y, Fujimura T, et al: **The effect of celecoxib, a cyclooxygenase-2 inhibitor, in familial adenomatous polyposis.** *N Engl J Med* 2000, **342**:1946–1952.
9. Phillips RK, Wallace MH, Lynch PM, Hawk E, Gordon GB, Saunders BP, Wakabayashi N, Shen Y, Zimmerman S, Godio L, et al: **A randomised, double blind, placebo controlled study of celecoxib, a selective cyclooxygenase 2 inhibitor, on duodenal polyposis in familial adenomatous polyposis.** *Gut* 2002, **50**:857–860.
10. Arber N, Spicak J, Racz I, Zavoral M, Breazna A, Gerletti P, Lechuga MJ, Collins N, Rosenstein RB, Eagle CJ, et al: **Five-year analysis of the prevention of colorectal sporadic adenomatous polyps trial.** *Am J Gastroenterol* 2011, **106**:1135–1146.
11. Solomon SD, McMurray JJ, Pfeffer MA, Wittes J, Fowler R, Finn P, Anderson WF, Zaubler A, Hawk E, Bertagnoli M: **Cardiovascular risk associated with celecoxib in a clinical trial for colorectal adenoma prevention.** *N Engl J Med* 2005, **352**:1071–1080.
12. Zell JA, Pelot D, Chen WP, McLaren CE, Gerner EW, Meyskens FL: **Risk of cardiovascular events in a randomized placebo-controlled, double-blind trial of difluoromethylornithine plus sulindac for the prevention of sporadic colorectal adenomas.** *Cancer Prev Res (Phila)* 2009, **2**:209–212.
13. Kim B, Giardiello FM: **Chemoprevention in familial adenomatous polyposis.** *Best Pract Res Clin Gastroenterol* 2011, **25**:607–622.
14. Fini L, Piazzi G, Daoud Y, Selgrad M, Maegawa S, Garcia M, Fogliano V, Romano M, Graziani G, Vitaglione P, et al: **Chemoprevention of intestinal polyps in ApcMin/+ mice fed with western or balanced diets by drinking annurca apple polyphenol extract.** *Cancer Prev Res (Phila)* 2011, **4**:907–915.
15. Rajput S, Mandal M: **Antitumor promoting potential of selected phytochemicals derived from spices: a review.** *Eur J Cancer Prev* 2012, **21**:205–215.
16. Woo CC, Kumar AP, Sethi G, Tan KH: **Thymoquinone: potential cure for inflammatory disorders and cancer.** *Biochem Pharmacol* 2012, **83**:443–451.
17. Li F, Rajendran P, Sethi G: **Thymoquinone inhibits proliferation, induces apoptosis and chemosensitizes human multiple myeloma cells through suppression of signal transducer and activator of transcription 3 activation pathway.** *Br J Pharmacol* 2010, **161**:541–554.
18. Yi T, Cho SG, Yi Z, Pang X, Rodriguez M, Wang Y, Sethi G, Aggarwal BB, Liu M: **Thymoquinone inhibits tumor angiogenesis and tumor growth through suppressing AKT and extracellular signal-regulated kinase signaling pathways.** *Mol Cancer Ther* 2008, **7**:1789–1796.
19. Das S, Dey KK, Dey G, Pal I, Majumder A, MaitiChoudhury S, Kundu SC, Mandal M: **Antineoplastic and apoptotic potential of traditional medicines thymoquinone and diosgenin in squamous cell carcinoma.** *PLoS One* 2012, **7**:e46641.
20. Gali-Muhtasib H, Ocker M, Kuester D, Krueger S, El-Hajj Z, Diestel A, Evert M, El-Najjar N, Peters B, Jurjus A, et al: **Thymoquinone reduces mouse colon tumor cell invasion and inhibits tumor growth in murine colon cancer models.** *J Cell Mol Med* 2008, **12**:330–342.
21. Gali-Muhtasib H, Diab-Assaf M, Boltze C, Al-Hmaira J, Hartig R, Roessner A, Schneider-Stock R: **Thymoquinone extracted from black seed triggers apoptotic cell death in human colorectal cancer cells via a p53-dependent mechanism.** *Int J Oncol* 2004, **25**:857–866.
22. Dang CV: **MYC on the path to cancer.** *Cell* 2012, **149**:22–35.
23. Klaus A, Birchmeier W: **Wnt signalling and its impact on development and cancer.** *Nat Rev Cancer* 2008, **8**:387–398.

24. da Costa LT, He TC, Yu J, Sparks AB, Morin PJ, Polyak K, Laken S, Vogelstein B, Kinzler KW: **CDX2 is mutated in a colorectal cancer with normal APC/ beta-catenin signaling.** *Oncogene* 1999, **18**:5010–5014.
25. Baker SJ, Markowitz S, Fearon ER, Willson JK, Vogelstein B: **Suppression of human colorectal carcinoma cell growth by wild-type p53.** *Science* 1990, **249**:912–915.
26. Welcker M, Orian A, Jin J, Grim JE, Harper JW, Eisenman RN, Clurman BE: **The Fbw7 tumor suppressor regulates glycogen synthase kinase 3 phosphorylation-dependent c-Myc protein degradation.** *Proc Natl Acad Sci USA* 2004, **101**:9085–9090.
27. Roepke M, Diestel A, Bajbouj K, Walluscheck D, Schonfeld P, Roessner A, Schneider-Stock R, Gali-Muhtasib H: **Lack of p53 augments thymoquinone-induced apoptosis and caspase activation in human osteosarcoma cells.** *Cancer Biol Ther* 2007, **6**:160–169.
28. El-Mahdy MA, Zhu Q, Wang QE, Wani G, Wani AA: **Thymoquinone induces apoptosis through activation of caspase-8 and mitochondrial events in p53-null myeloblastic leukemia HL-60 cells.** *Int J Cancer* 2005, **117**:409–417.
29. Gali-Muhtasib H, Kuester D, Mawrin C, Bajbouj K, Diestel A, Ocker M, Habold C, Foltzer-Jourdainne C, Schoenfeld P, Peters B, et al: **Thymoquinone triggers inactivation of the stress response pathway sensor CHEK1 and contributes to apoptosis in colorectal cancer cells.** *Cancer Res* 2008, **68**:5609–5618.
30. Li Y, Bharti A, Chen D, Gong J, Kufe D: **Interaction of glycogen synthase kinase 3beta with the DF3/MUC1 carcinoma-associated antigen and beta-catenin.** *Mol Cell Biol* 1998, **18**:7216–7224.
31. Houghton PJ, Zarka R, HB DI, Hoult JR: **Fixed oil of Nigella sativa and derived thymoquinone inhibit eicosanoid generation in leukocytes and membrane lipid peroxidation.** *Planta Med* 1995, **61**:33–36.
32. Burits M, Bucar F: **Antioxidant activity of Nigella sativa essential oil.** *Phytother Res* 2000, **14**:323–328.
33. Reagan-Shaw S, Nihal M, Ahmad N: **Dose translation from animal to human studies revisited.** *FASEB J* 2008, **22**:659–661.
34. Salem EM, Yar T, Bamosa AO, Al-Quorain A, Yasawy MI, Alsulaiman RM, Randhawa MA: **Comparative study of Nigella Sativa and triple therapy in eradication of Helicobacter Pylori in patients with non-ulcer dyspepsia.** *Saudi J Gastroenterol* 2010, **16**:207–214.
35. Bamosa AO, Kaatabi H, Lebdaa FM, Elq AM, Al-Sultanb A: **Effect of Nigella sativa seeds on the glycemic control of patients with type 2 diabetes mellitus.** *Indian J Physiol Pharmacol* 2010, **54**:344–354.
36. Badary OA, Al-Shabanah OA, Nagi MN, Al-Bekairi AM, Elmazar MMA: **Acute and subchronic toxicity of thymoquinone in mice.** *Drug Dev Res* 1998, **44**:56–61.
37. Khalife KH, Lupidi G: **Reduction of hypervalent states of myoglobin and hemoglobin to their ferrous forms by thymoquinone: the role of GSH, NADH and NADPH.** *Biochim Biophys Acta* 2008, **1780**:627–637.
38. Su LK, Kinzler KW, Vogelstein B, Preisinger AC, Moser AR, Luongo C, Gould KA, Dove WF: **Multiple intestinal neoplasia caused by a mutation in the murine homolog of the APC gene.** *Science* 1992, **256**:668–670.
39. Musteanu M, Blaas L, Mair M, Schlederer M, Bilban M, Tauber S, Esterbauer H, Mueller M, Casanova E, Kenner L, et al: **Stat3 is a negative regulator of intestinal tumor progression in Apc(Min) mice.** *Gastroenterology* 2010, **138**:1003–1011.
40. Ritland SR, Gendler SJ: **Chemoprevention of intestinal adenomas in the ApcMin mouse by piroxicam: kinetics, strain effects and resistance to chemosuppression.** *Carcinogenesis* 1999, **20**:51–58.
41. Jacoby RF, Marshall DJ, Newton MA, Novakovic K, Tutsch K, Cole CE, Lubet RA, Kelloff GJ, Verma A, Moser AR, et al: **Chemoprevention of spontaneous intestinal adenomas in the Apc Min mouse model by the nonsteroidal anti-inflammatory drug piroxicam.** *Cancer Res* 1996, **56**:710–714.
42. Moser AR, Mattes EM, Dove WF, Lindstrom MJ, Haag JD, Gould MN: **ApcMin, a mutation in the murine Apc gene, predisposes to mammary carcinomas and focal alveolar hyperplasias.** *Proc Natl Acad Sci USA* 1993, **90**:8977–8981.
43. Becker C, Fantini MC, Wirtz S, Nikolaev A, Kiesslich R, Lehr HA, Galle PR, Neurath MF: **In vivo imaging of colitis and colon cancer development in mice using high resolution chromoendoscopy.** *Gut* 2005, **54**:950–954.
44. Moolenbeek C, Ruitenber EJ: **The "Swiss roll": a simple technique for histological studies of the rodent intestine.** *Lab Anim* 1981, **15**:57–59.
45. Boivin GP, Washington K, Yang K, Ward JM, Pretlow TP, Russell R, Besselsen DG, Godfrey VL, Doetschman T, Dove WF, et al: **Pathology of mouse models of intestinal cancer: consensus report and recommendations.** *Gastroenterology* 2003, **124**:762–777.
46. Lopez DS I, Fan J, Yang X, Zonderman AB, Potapova O, Pizer ES, Gorospe M: **Role of the RNA-binding protein HuR in colon carcinogenesis.** *Oncogene* 2003, **22**:7146–7154.
47. Roig AI, Eskiocak U, Hight SK, Kim SB, Delgado O, Souza RF, Spechler SJ, Wright WE, Shay JW: **Immortalized epithelial cells derived from human colon biopsies express stem cell markers and differentiate in vitro.** *Gastroenterology* 2010, **138**:1012–1021.
48. Campregher C, Schmid G, Ferk F, Knasmuller S, Khare V, Kortum B, Dammann K, Lang M, Scharl T, Spittler A, et al: **MSH3-Deficiency Initiates EMAS without Oncogenic Transformation of Human Colon Epithelial Cells.** *PLoS One* 2012, **7**:e50541.
49. Lee JH, Kang Y, Khare V, Jin ZY, Kang MY, Yoon Y, Hyun JW, Chung MH, Cho SI, Jun JY, et al: **The p53-inducible gene 3 (PIG3) contributes to early cellular response to DNA damage.** *Oncogene* 2010, **29**:1431–1450.
50. Howard S, Deroo T, Fujita Y, Itasaki N: **A positive role of cadherin in Wnt/beta-catenin signalling during epithelial-mesenchymal transition.** *PLoS One* 2011, **6**:e23899.
51. Pfaffl MW: **A new mathematical model for relative quantification in real-time RT-PCR.** *Nucleic Acids Res* 2001, **29**:e45.

doi:10.1186/1476-4598-12-41

Cite this article as: Lang et al.: Thymoquinone attenuates tumor growth in Apc^{Min} mice by interference with Wnt-signaling. *Molecular Cancer* 2013 **12**:41.

Submit your next manuscript to BioMed Central and take full advantage of:

- Convenient online submission
- Thorough peer review
- No space constraints or color figure charges
- Immediate publication on acceptance
- Inclusion in PubMed, CAS, Scopus and Google Scholar
- Research which is freely available for redistribution

Submit your manuscript at
www.biomedcentral.com/submit

